Quasi–Linear Regime of Gravitational Instability: Implication to Density–Velocity Relation

Sergei F. Shandarin
Department of Physics and Astronomy
University of Kansas
Lawrence, Kansas 66045, USA

To appear in the Proceedings of
the Conference "Cosmic Velocity Fields"
Paris, July 1993

QUASI-LINEAR REGIME OF GRAVITATIONAL INSTABILITY: IMPLICATION TO DENSITY-VELOCITY RELATION

S.F. SHANDARIN
Department of Physics and Astronomy, University of Kansas, Lawrence, KS 66045

Abstract

The well known linear relation between density and peculiar velocity distributions is a powerful tool for studying the large-scale structure in the Universe. Potentially it can test the gravitational instability theory and measure Ω. At present it is used in both ways: the velocity is reconstructed provided the density is given and vice versa. Reconstructing the density from the velocity field usually makes use of the Zel'dovich approximation. However, the standard linear approximation in Eulerian space is used when the velocity is reconstructed from the density distribution. I show that the linearized Zel'dovich approximation, in other words the linear approximation in the Lagrangian space, is more accurate for reconstructing velocity. In principle, a simple iteration technique can recover both the density and velocity distributions in Lagrangian space, but its practical application may need an additional study.

1 Introduction

In this talk I would like to discuss the quasi-linear regime of the gravitational instability and in particular the density-velocity relation. This is the relation between peculiar velocity $\mathbf{v}_p(\mathbf{x})$ and density contrast $\delta(\mathbf{x})$. The peculiar velocity is defined as

$$\mathbf{v}_p(\mathbf{x},t) \equiv a\frac{d\mathbf{x}}{dt} \ , \tag{1}$$

where $\mathbf{x} = \mathbf{r}/a$ is a comoving coordinate and $a = a(t)$ is the scale factor. The density contrast is the relative density perturbation

$$\delta(\mathbf{x},t) \equiv \frac{\rho(\mathbf{x},t) - \bar{\rho}}{\bar{\rho}}. \tag{2}$$

The equation relating peculiar velocity $\mathbf{v}_p$ and the density contrast δ is derived, for example, in [8])

$$\mathbf{v}_p(\mathbf{x}) = \frac{H f a}{4\pi}\int \delta(\mathbf{x}')\frac{\mathbf{x}'-\mathbf{x}}{\mid \mathbf{x}'-\mathbf{x} \mid^3}d^3x' \tag{3}$$

where $H = \dot{a}/a$ is the Hubble constant, $f \equiv \frac{a}{D}\frac{dD}{da}$, and D is the growth factor of density fluctuations $\delta \propto D(t)$; in the $\Omega = 1$ matter dominated cosmology $D \propto a \propto t^{2/3}$. Eq.(3) is widely used for reconstruction of velocity field from density field (see e.g., [10]). Quantitatively eq.(3) is valid only in the linear regime which is based on two assumptions: (1) $\delta << 1$ and (2)$\mathbf{x} \simeq \mathbf{q}$, where $\mathbf{q}$ is the unperturbed (Lagrangian) comoving coordinate of the particle. The generalization of relation (3)

including the nonlinear corrections to δ was studied in [7]. The second assumption is a subject of the paper. To stress this assumption we obtain an analog of eq.(3) from the Zel'dovich approximation [12], [11]. The Zel'dovich approximation is usually formulated as a relation between the comoving Eulerian $\mathbf{x}$ and Lagrangian $\mathbf{q}$ coordinates of particles

$$\mathbf{x} = \mathbf{q} + D(t) \cdot \mathbf{s}(\mathbf{q}) \,, \tag{4}$$

where $\mathbf{s}(\mathbf{q}) = - \bigtriangledown \varphi_0(\mathbf{q})$ is the potential vector field characterizing the growing mode of the initial perturbations. The density can be found in terms of the eigenvalues $\lambda_1(\mathbf{q})$, $\lambda_2(\mathbf{q})$, $\lambda_3(\mathbf{q})$ of the initial deformation tensor field $d_{ik}(\mathbf{q}) = -\partial s_i/\partial q_k$

$$\rho(\mathbf{q},t) = \frac{\bar{\rho}}{(1-D\lambda_1)(1-D\lambda_2)(1-D\lambda_3)} \tag{5}$$

and the peculiar velocity field in terms of $\mathbf{s}(\mathbf{q})$

$$\mathbf{v}_p(\mathbf{q},t) = a\dot{D}\mathbf{s}(\mathbf{q}). \tag{6}$$

In the limit $\mid D\lambda_i \mid << 1$ eq.(5) reduces to

$$\delta(\mathbf{q},t) = -D\frac{\partial s_i}{\partial q_i}, \tag{7}$$

where $\partial s_i/\partial q_i = \lambda_1 + \lambda_2 + \lambda_3$. Solving eq.(7) together with eq.(6) we readily obtain the desired Lagrangian analog of eq.(3)

$$\mathbf{v}_p(\mathbf{q},a) = \frac{H\,f\,a}{4\pi}\int \delta(\mathbf{q}')\frac{\mathbf{q}'-\mathbf{q}}{\mid \mathbf{q}'-\mathbf{q} \mid^3} d^3q' \,. \tag{8}$$

The only difference between (3) and (8) is the difference between Eulerian coordinates $\mathbf{x}$ and Lagrangian coordinates $\mathbf{q}$. One might think that at small δ the difference between Eulerian and Lagrangian coordinates always can be neglected. This assumption being right for some spectra is generally wrong and it is the major subject of this talk.

2 Three regimes of gravitational instability

A very useful theoretical model for studying the formation and properties of the large scale structure is a dust like continuous medium described in great detail in [8]. The equations describing the evolution of density perturbations in this model can be conveniently written in a slightly different form

$$\frac{\partial \eta}{\partial D} + \frac{\partial(\eta \cdot v_i)}{\partial x_i} = 0 \tag{9}$$

$$\frac{\partial v_i}{\partial D} + v_k\frac{\partial v_i}{\partial x_k} = \frac{3}{2}\frac{\Omega}{D \cdot f^2}(\frac{\partial \varphi}{\partial x_i} + v_i) \tag{10}$$

$$\frac{\partial^2 \varphi}{\partial x_i^2} = \frac{\delta}{D} \tag{11}$$

$$\eta = \bar{\eta}(1+\delta), \tag{12}$$

where as usually $x_i = r_i/a$ is the comoving coordinate, but the peculiar velocity is *scaled* by the first derivative of the growth factor $v_i = v_{pi}/(a \cdot \dot{D}) = \dot{D}^{-1} \cdot dx_i/dt = dx_i/dD$, $\eta = \rho \cdot a^3$, and the perturbation of the gravitational potential $\varphi_g = 3/2\Omega\dot{a}^2 D \cdot \varphi$.

The standard gravitational instability paradigm usually assumes that the evolution of the density perturbations having a comoving scale L has two stages: the linear stage when $\sigma_\rho(L) < 1$ or equivalently $L > 1/k_{nl}$ and afterward the nonlinear stage when $\sigma_\rho(L) > 1$ and $L < 1/k_{nl}$, where k_{nl} is defined by the condition

$$\sigma_\rho^2(k_{nl}^{-1}) = 4\pi \cdot D^2 \int_0^{k_{nl}} P(k)k^2 dk = 1. \tag{13}$$

I show that for some initial spectra an additional stage which can be called the quasi-linear regime can be identified. For such a spectra the difference between the Eulerian (r_i) and Lagrangian (q_i) coordinates is significant and can influence the density-velocity relation.

2.1 Linear regime

The evolution of the scales which are in the linear regime can be described by a set of simple linear equations. Linearizing eq.(9) and (10) we obtain

$$\frac{\partial \delta}{\partial D} = -\frac{\partial v_i}{\partial x_i} \approx \delta_0(\mathbf{x}), \tag{14}$$

$$\frac{\partial v_i}{\partial D} = 0. \tag{15}$$

The well known growing solution of this system in our variables takes a form

$$\delta(\mathbf{x}, D) = D \cdot \delta_0(\mathbf{x}), \tag{16}$$

$$v_i(\mathbf{x}, D) = v_{0i}(\mathbf{x}), \tag{17}$$

$$\varphi(\mathbf{x}) = \varphi_0(\mathbf{x}), \tag{18}$$

where $\delta_0(\mathbf{x})$, $v_{0i}(\mathbf{x})$ and $\varphi_0(\mathbf{x})$ are the initial density, velocity and gravitational potential (scaled as was indicated above) perturbations. The growing mode is specified by only one spatial function, so the initial density, velocity and potential are related as $v_{0i}(\mathbf{x}) = -\frac{\partial \varphi_0}{\partial x_i}$ and $\delta_0(\mathbf{x}) = -\frac{\partial v_{0i}}{\partial x_i}$. From this solution one can see that it preserves the initial spatial structure of the perturbation. In other words this approximation ignores the fact that the growth of the amplitude of the perturbation requires the displacement of mass. The linear approximation can be used quantitatively only when $\delta \ll 1$, but in practice it is often pushed to the limit $\delta \approx 1$. However, a simple order of magnitude analysis suggests that in some cases there is an additional condition restricting the linear approximation in the above form.

The continuity equation (eq.(9)) can also be written in terms of the density contrast

$$\frac{\partial \delta}{\partial D} + \frac{\partial v_i}{\partial x_i} + v_i \frac{\partial \delta}{\partial x_i} + \delta \frac{\partial v_i}{\partial x_i} = 0. \tag{19}$$

For the order of magnitude estimates we replace the derivatives by the finite ratios

$$\delta/D + v/l_v + v(\delta/l_\delta) + \delta(v/l_v) \sim 0. \tag{20}$$

Here v is the characteristic fluid velocity and l_δ, l_v are the coherence lengths for spatial variations of δ and v respectively. Comparing linear eq.(14) with the exact continuity equation (19) one can see that two last terms were discarded from eq.(19). The order of magnitude estimate of eq.(14) simply yields $\delta \sim D \cdot (v/l_v)$ which is of course in agreement with solution (16).

Making use of eq.(20) we readily find that the last term in eq.(19) can be neglected if the density contrast is small $\delta < 1$ or equivalently $D < l_v/v$.

However, discarding the third term of eq.(19) requires a condition $\delta < l_\delta/l_v$ or equivalently $D < l_\delta/v$ which may be much stronger: if $l_\delta \ll l_v$ then the linear theory is correct only until $\delta < l_\delta/l_v \ll 1$.

Discarding the second term on the left hand side of the Euler equation (eq.(10)) is justified if $D < l_v/v$ which coincides with the requirement for the density contrast to be small. The right hand side of the Euler equation is zero to the linear order. Of course, using the linear theory for a quantitative analysis all signs "<" in the above inequalities must be replaced by "$\ll$".

In a simple case when $l_\delta \sim l_v$ the linear approximation can be used for a qualitative analysis up to the beginning of the nonlinear stage $\delta \approx 1$. The relation between l_δ and l_v is determined by the initial spectrum and will be discussed later.

The Fourier components $\delta_{\mathbf{k}}$ of the perturbations in the linear regime grow linearly and the phases $\psi_{\mathbf{k}}$ remain constant

$$\delta_{\mathbf{k}}(D) \approx D \cdot \delta_{\mathbf{k}}(0) \tag{21}$$

$$\psi_{\mathbf{k}}(D) \approx \psi_{\mathbf{k}}(0). \tag{22}$$

2.2 Nonlinear regime

The perturbations with scales smaller than k_{nl}^{-1} are in the nonlinear regime. The analysis of the nonlinear perturbations requires solving the full nonlinear equations (9-12) which at present is not possible in a general case. In a few cases when a particular type of symmetry is imposed (e.g. spherical) the exact solutions are known. For the random initial conditions the hierarchical clustering model gives a good qualitative and in some cases quantitative description of the process (for details see, e.g. [8] and references therein). In the nonlinear regime both equalities eq.(21) and (22) break

$$\delta_{\mathbf{k}}(D) \neq D \cdot \delta_{\mathbf{k}}(0)$$

$$\psi_{\mathbf{k}}(D) \neq \psi_{\mathbf{k}}(0).$$

The growth of the amplitude slows down and the growth of the density perturbations is determined mostly by the phase adjusting.

2.3 Quasi-linear regime

Two nonlinear terms $v_i \frac{\partial \delta}{\partial x_i}$ dropped from the continuity equation (eq.(19)) and $v_k \frac{\partial v_i}{\partial x_k}$ dropped from the Euler equation (eq.(10)), when linearizing the original equations, can be relatively easy retained

$$\frac{\partial \delta}{\partial D} + v_i \frac{\partial \delta}{\partial x_i} = \delta_0(\mathbf{x})$$

$$\frac{\partial v_i}{\partial D} + v_k \frac{\partial v_i}{\partial x_k} = 0.$$

$$\varphi(\mathbf{x}) = \varphi_0(\mathbf{x}).$$

This set of partly linearized equations differs from one usually used in the linear analysis. In the Lagrangian form these nonlinear terms can be absorbed into the time derivative retaining linearity

$$\frac{d\delta}{dD} = \delta_0(\mathbf{q})$$

$$\frac{dv_i}{dD} = 0.$$

The solution to this system is obvious:

$$\delta(\mathbf{x}, D) = D \cdot \delta_0(\mathbf{q}), \tag{23}$$

$$v_i(\mathbf{x}, D) = v_{0i}(\mathbf{q}). \tag{24}$$

Solution (23, 24) looks similar to (16, 17), but must be interpreted differently. It does not describe the 'real' distribution of density and velocity in space, instead it describes them in the Lagrangian space. However, we may find the 'real' (Eulerian) distributions assigning the density and velocity values of eq.(23, 24) to the coordinates $x_i = q_i + D \cdot v_{0i}(\mathbf{q})$, provided that $x_i = q_i$ at $D = 0$. The last equation is, of course, the Zel'dovich approximation eq.(4) with $s_i = v_{0i}$. The difference between the Lagrangian coordinate q_i and the Eulerian coordinate x_i can be unimportant, for instance, if we are interested in the internal structure of clumps, or their integral properties like masses, or angular momenta. However, it is crucial if the goal is the spatial distribution of the clumps or the velocity on scales of tens of Mpc.. Passing by we note that the Zel'dovich approximation is actually an extrapolation of solution (4) until the shell crossing. Formally it is not accurate even to the second order, but practically is quite good [2], [11].

The difference between Eulerian and Lagrangian coordinates comprises the difference between the linear and quasi-linear regimes.

In terms of the Fourier components the qasi-linear regime is a mixture of the linear and nonlinear cases. The Fourier components grow approximately according to the linear theory (eq.(21)) and the phases are very different from the initial ones

$$\delta_{\mathbf{k}}(D) \approx D \cdot \delta_{\mathbf{k}}(0),$$

$$\psi_{\mathbf{k}}(D) \neq \psi_{\mathbf{k}}(0).$$

An immediate question arises: which scales are in the quasi-linear regime? The answer comes from our order of magnitude analysis: the scales in the quasi-linear regime are those which on the one hand are greater than the nonlinear scale eq.(13) and on the other hand are smaller than the typical displacement of a particle from its unperturbed position (Lagrangian coordinate) to the current position (Eulerian coordinate). Ryden and Gramann [9] found in two-dimensional N-body simulations that the scale where the phases become substantially different from the initial ones in some cases does not scale with k_{nl}. As the author checked it perfectly scales with the theoretically calculated characteristic displacement of mass.

3 Characteristic displacement of mass

For estimation ot the mean distance passed by the mass one can use the Zel'dovich approximation eq.(4)

$$d_{rms} \equiv < (\mathbf{x} - \mathbf{q})^2 >^{1/2} = D(t) \cdot s_{rms}$$

where

$$s_{rms} \equiv < \mathbf{s}^2(\mathbf{q}) >^{1/2} \tag{25}$$

However eq.(4) holds only before crossing of the orbits. To make use of relation (4) at later times one can smooth initial perturbation field at k_{nl} which is defined by eq.(13). Then

$$s^2_{rms}(k_{nl}) = 4\pi \int_0^{k_{nl}} P(k)dk. \tag{26}$$

Combining eq.(25), (13) and (26) we may express the r.m.s. distance in terms of the initial power spectrum

$$d^2_{rms}(k_{nl}) = \frac{\int_0^{k_{nl}} P(k)dk}{\int_0^{k_{nl}} P(k)k^2dk}. \tag{27}$$

Obviously integrals in eq.(27) could be easily defined in terms of an arbitrary (e.g., Gaussian) smoothing window function. Pushing the upper limits in eq.(27) to the infinity one obtains the familiar characteristic scale of the initial vector field $\mathbf{s}(\mathbf{q})$. On the other hand, the r.m.s. displacement is always equal to the characteristic scale of the initial velocity field smoothed with the scale on nonlinearity. Before going to implications of eq.(27) it is worth discussing its accuracy. One obvious test of eq.(27) is its comparison with N-body simulations. This test has been carried out for a series of power law models.

3.1 Power law spectra

Pure power law initial spectra play a very important theoretical role since they have various scaling properties. Here I discuss slightly modified power law models imposing explicitly a cutoff k_1 at small k corresponding to the large scales. This modification solves the problem of divergence at large scales for certain spectra. The cutoff is arbitrary and can be treated as a free parameter. The limiting case of a pure power law can be analyzed assuming an obvious limit $k_1 \to 0$. All N–body simulations assume a sharp cutoff of the initial spectrum at the fundamental mode $k_f = 2\pi/L_{box}$. Therefore this theoretical model better suits the purpose of explaining the results of N–body simulations.

The initial spectrum has a form

$$P(k) = \begin{cases} A_n k^n, & k \geq k_1 \\ 0\,, & k < k_1 \end{cases} \tag{28}$$

where A_n is a constant. Assuming the linear growth of the amplitude of density perturbation at $k \leq k_{nl}$ eq.(21) one can easily find the nonlinear scale

$$k_{nl} = \left(\frac{n+3}{4\pi A_n D^2} + k_1^{n+3} \right)^{\frac{1}{n+3}}; n > -3.$$

Assuming $k_{nl} >> k_1$ one obtains a familiar result [8]

$$k_{nl} \propto D^{-2/(n+3)}; n > -3\,,$$

which tells us that the scale of nonlinearity monotonically grows with time if $n > -3$. This is usually interpreted as hierarchical clustering of smaller nonlinear clumps into larger ones. The typical mass of clumps formed can be estimated as

$$M_{nl} \sim \bar{\rho} \frac{4\pi}{3} k_{nl}^{-3} \propto D^{6/(n+3)}; n > -3. \tag{29}$$

It is also assumed that a substantial fraction of mass (~ 0.5) is in such clumps. Obviously, for making such a clumps it is sufficient to move mass over a distance about k_{nl}^{-1}. On the other hand applying eq.(27) with the lower limits at $k = k_1$ to spectra eq.(28) one easily obtains in the limits $k_{nl} >> k_1$

$$d_{rms}(k_{nl}) = \begin{cases} \sqrt{\frac{n+3}{n+1}} \frac{1}{k_{nl}}\,, & n > -1 \\ \sqrt{2\ell n \frac{k_{nl}}{k_1}} \frac{1}{k_{nl}}\,, & n = -1 \\ \sqrt{-\frac{n+3}{n+1}} \left(\frac{k_1}{k_{nl}} \right)^{\frac{n+1}{2}} \frac{1}{k_{nl}} & -1 > n > -3 \end{cases} \tag{30}$$

At $n > -1$ d_{rms} is about k_{nl}, however at $n \leq -1$ the $r.m.s.$ distance can be much greater than k_{nl}^{-1} depending on k_1. This means that in the case $-3 \leq n \leq -1$ the clumps with masses $\sim M_{nl}$ (eq.(29)) move coherently, and as we commented before the coherence scale of this motion always about d_{rms}. If the initial spectrum is even steeper $n < -3$ then no clumps form, until the first pancakes are formed.

3.2 Comparison with N-body simulations

Prediction of eq.(27) was tested in a series of 3 dimensional N-body simulations. The simulations [3] were done with 128^3 particles on equal mesh for five power law initial spectra eq.(28) with $n = 1, 0, -1, -2, -3$ and $k_1 = k_f = 2\pi/L_{box}$ each model was simulated with three different sets of random numbers. Each simulation was stopped when $k_{nl} = 64, 32, 16, 8$ and 4 and $d_{rms}(N - body)$ was calculated from the particle distribution

$$d_{rms}\Big(N - \text{body}\Big) = < (\mathbf{r}_i - \mathbf{q}_i)^2 >^{1/2} \quad .$$

The results in mesh units are shown in Figure 1. Along with the experimental points the analytic calculations using eq.(27) with the lower limit $k = k_f$ are also shown with dashed lines ($n = 1, 0, -1, -2, -3$ from the bottom to top). The solid line shows relation $d_{rms} = k_{nl}^{-1}$. Three symbols of the same type at given k_{nl} corresponds to different realization of random numbers. For $n = 1$ (open triangles) and $n = 0$ (open squares) the results for different realizations almost coincide with each other so fewer than three symbols can be seen. The $n = -3, -2, -1$ series are almost exactly coincide with the theoretical predictions for all k_{nl} from $64k_f$ to $4k_f$. The agreement between the theory and the experiments gets worse for the $n = 0$ and especially for the $n = 1$ series. Actually it is not unexpected. According to eq.(30) for the $n = 1$ and $n = 0$ models d_{rms} is only 1.4 and 1.7 times greater than k_{nl}^{-1} therefore the accuracy of the essentially linear theory can not be very good. However, even for these spectra in the worst case the discrepancy does not exceed about 40%. Applying the theory to cosmology one has to keep in mind that all realistic models of the large scale structure based on gravitational instability suggest that the present nonlinear scale is in the region where the initial spectrum had effective slope about $n \simeq -1$ or even steeper. For such spectra the accuracy of eq.(27) is far better. In any case it gives a good lower limit for d_{rms}.

3.3 CDM spectrum

The initial spectrum of perturbations might not be a pure power law. A good realistic test model is the CDM spectrum. In this case a numerical evaluation of the integrals in eq.(27) is needed. The typical normalization $k_{nl}^{-1} \approx 4.5h^{-1}Mpc$ roughly corresponding to the COBE normalization of the primordial spectrum gives $d_{rms}(CDM) \approx 9h^{-1}Mpc \approx 900km/s$.

4 Discussion

The growth of the density perturbations necessarily assumes the displacement of mass. A good estimate of the typical distance traveled by a particle (e.g. a galaxy) from its unperturbed position can be given analytically applying the Zel'dovich approximation to the initial power spectrum truncated at the nonlinear scale eq.(27). The comparison with the three-dimensional N-body simulations carried out for five power law models with $n = -3, -2, -1, 0, 1$ showed that eq.(27) is almost exact if $n \leq -1$ and for $n = 0$ and 1 the actual displacement is about 20-40% greater than the analytical prediction. Actually, the density distribution predicted by the truncated Zel'dovich approximation is far better than all other tested analytical or semianalytical approximation (see [1], [4], [5], [6]).

For the CDM spectrum (taken here as an example) with the COBE normalization the theory predicts the characteristic displacement of about $900km/s$. The statistic of the displacement is roughly Gaussian, which means that more than 30% of the mass as well as of galaxies has been displaced even more. It implys that the standard linear relation between δ and $\mathbf{v}_p$ eq.(3) can result in a large error unless the smoothing scale is greater than at least $1000km/s$.

Smoothing effectively reduces the difference between the Eulerian and Lagrangian coordinates and with a sufficiently large smoothing scales it can be completely erased. However, the displacement

pattern due to gravitational instability is not identical to that of smoothing, therefore a reasonable quantitative agreement between the Eulerian and Lagrangian distributions may require even a larger smoothing scale. For example, the analysis of the nonlinear Eulerian and correspondingly scaled initial Lagrangian density distributions smoothed with the same Gaussian window showed that only when the size of the window reaches $R_w \approx 1.65 d_{rms}$ the r.m.s. difference between the two density fields becomes about 25% almost independently of the initial spectrum [3]. Applying this result to the CDM model we find that for obtaining a density field for the density- velocity relation eq.(3) with 25% accuracy the original density field must be smoothed with a scale at least $1500 km/s$.

A similar problem arises when a reconstruction technique is tested in an N-body simulations. If the r.m.s. displacement of particles in the simulation is smaller than in the tested theory or the universe (e.g. because the box is too small) then the technique will look better in the numerical test compared to its performance in the theory or on real data.

The above constraint seems not to be a problem for the POTENT which employs the Zel'dovich (or modified Zel'dovich) approximation, but for the reconstruction of the peculiar velocity field from the density distribution may suffer from this effect.

An obvious way of eliminating this effect consists in recovering the Lagrangian coordinates. One may start from the original density field and find the first approximation to the peculiar velocity field using eq.(3). Next, the density must be assigned to the Lagrangian coordinates which can be found from the reverse Zel'dovich approximation $q_i = x_i - D \cdot v_i$. After that, the whole procedure must be repeated again, but this time eq.(8) must be used. Iterating, one can get the Lagrangian distributions with desired accuracy. Unfortunately this method requires the knowledge of the factor D which in turn depends on Ω and the normalization of the primordial spectrum.

Acknowledgements. I am grateful for financial support from NASA Grant NAGW-2923, NSF Grants AST-9021414 and OSR-9255223, and the University of Kansas GRF fund.

References

[1] Coles, P., Melott, A., & Shandarin, S. 1993. *Mon. Not. R. astr. Soc* **260**, 765

[2] Doroshkevich, A., Ryabenki, V., & Shandarin, S. 1973. *Astrophysics* **9**, 144

[3] Melott, A., & Shandarin, S. 1993. *Astrophys. J.* **410**, 469

[4] Melott, A., Pellman, T., & Shandarin, S. 1993. *Mon. Not. R. astr. Soc* submitted

[5] Melott, A., Shandarin, S., & Weinberg, D. 1993. in preparation

[6] Melott, A., Lucchin, F., Matarrese, S., & Moscardini, L. 1993, *Mon. Not. R. astr. Soc* submitted

[7] Nusser, & Dekel, A., Bertschinger, E., & Blumenthal, G. 1991. *Astrophys. J.* **379**, 6

[8] Peebles, P.J.E. 1980. The Large-Scale Structure of the Universe, Princeton University Press, Princeton

[9] Ryden, B., & Gramann, M. 1991. *Astrophys. J.* **383**, L33

[10] Strauss, M., Yahil, A., Davis, M., Huchra, J., & Fisher, K. 1992. *Astrophys. J.* **397**, 395 *Astrophys. J.* **361**, 49

[11] Shandarin, S.F., & Zel'dovich, Ya.B. 1989. *Rev. Mod. Phys.* **61**, 185

[12] Zel'dovich, Ya.B. 1970. *Astr. Astrophys.* **5**, 84

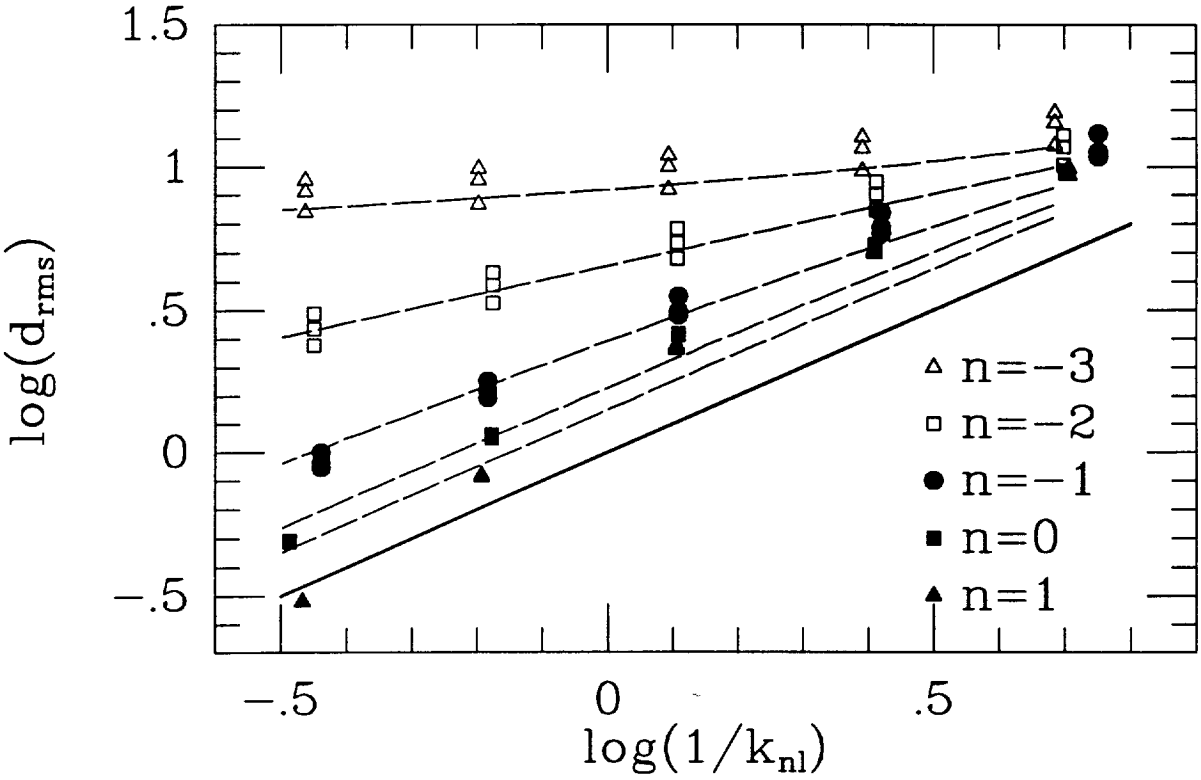

Fig.1 d_{rms} as a function of the nonlinear scale. Points are results of the N−body simulation. Dashed lines are the theoretical curves. A solid line shows $d_{rms} = 1/k_{nl}$.